ELSEVIER

Journal of Membrane Science 121 (1996) 11–24

journal of MEMBRANE SCIENCE

Approximate modeling of spiral-wound gas permeators

Runhong Qi, Michael A. Henson *

Department of Chemical Engineering, Louisiana State University, Baton Rouge, LA 70803-7303, USA

Received 21 March 1996; revised 13 May 1996; accepted 13 May 1996

Abstract

An approximate modeling technique for spiral-wound permeators separating binary gas mixtures is developed. The approximate model is derived directly from a standard fundamental model [1] by assuming that the residue flow rate is constant in the direction of permeate flow. This assumption reduces the original boundary value problem to a more computationally tractable problem involving a small number of nonlinear algebraic equations. Theoretical justification for the modeling technique is obtained via comparison to one-point collocation. A nonlinear programming method for estimating unknown model parameters from experimental data is proposed. The approximate modeling and parameter estimation techniques are evaluated for the separation of CO_2/CH_4 mixtures.

Keywords: Gas separations; Gas and vapor permeation; Modules; Modeling

1. Introduction

Over the past fifteen years, membrane systems have become viable alternatives to conventional gas separation processes such as amine adsorption and cryogenic distillation [2]. The emergence of gas separation membranes is due primarily to three critical developments: (*i*) synthesis of high performance polymer membrane materials [3]; (*ii*) large scale production techniques for high flux asymmetric membranes [4]; and (*iii*) fabrication techniques for high surface area membrane permeators [5]. As noted by Spillman [2], the economic viability of membrane separation processes also depends critically on process design. A major obstruction to effective design is the lack of appropriate permeator models.

A wide variety of permeator models have been proposed for both binary and multicomponent separations [6]. For the most part, available models differ according to assumptions about the flow pattern and the permeate-side pressure drop. Models based on the assumption of complete mixing on both sides of the membrane consist of simple nonlinear algebraic equations [7,8]. However, such models are not sufficiently accurate for process design since complete mixing is rarely achieved in practice. Models based on plug-flow and cross-flow patterns are comprised of coupled, nonlinear ordinary differential equations that usually yield boundary value problems [1,9–11]. While such models offer improved accuracy as compared to complete mixing models, they are likely to result in prohibitive computational requirements when utilized for process design.

An alternative approach is to develop approximate permeators models that offer a better tradeoff between prediction accuracy and computational com-

* Corresponding author. Tel.: 504-388-3690; E-mail: henson@nlc.che.lsu.edu.

PII S0376-7388(96)00156-1

plexity. The driving force approximation method [12] is based on the assumption that the driving force for permeation varies quadratically with membrane area. This assumption yields a nonlinear algebraic equation model that can be efficiently solved to predict permeator performance. However, the model may not converge [13] and is not applicable to the cross-flow pattern present in spiral-wound permeators. Pettersen and Lien [13] recently proposed an alternative modeling approach for gas permeators analogous to that commonly used for heat exchangers. The model describes the component fluxes across the membrane in terms of log mean partial pressure differences. However, the model is restricted to hollow fiber permeators and is based on several unrealistic assumptions including constant permeate-side pressure. Other approximate models [6,14,15] suffer from similar disadvantages.

In this paper, we propose an approximate modeling technique for spiral-wound permeators separating binary gas mixtures. The model is based on the assumption that the residue flow rate does not vary in the direction of permeate flow. By applying this assumption to a standard fundamental model [1], the original boundary value problem is reduced to a much simpler set of nonlinear algebraic equations. Because the resulting model may contain several unknown parameters, a simple and efficient strategy for estimating model parameters from experimental data is developed. The accuracy of the approximate model is evaluated by comparing the predictions with those obtained from the fundamental model for a wide range of CO_2/CH_4 separations.

2. Fundamental model

First we present the fundamental model of a spiral-wound gas permeator proposed by Pan [1]. The model development is based on Fig. 1, which depicts permeation through an extended membrane leaf of a spiral-wound permeator. The notation is defined in the List of Symbols. The leaf is comprised of two asymmetric membranes separated by a spacing material. Three edges of the leaf are sealed and the open edge is attached to a perforated tube. The feed stream is introduced on the outside of the leaf, and gas permeates through both of the membranes

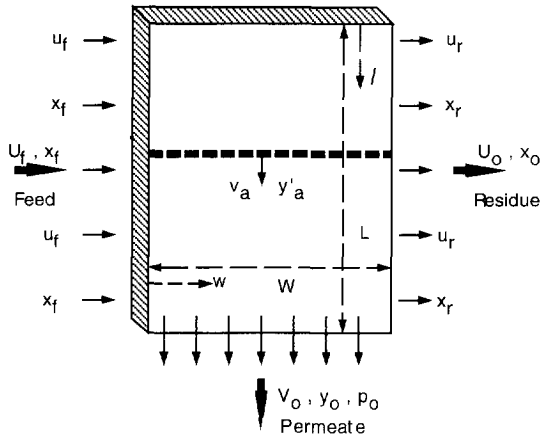

Fig. 1. Gas permeation through a spiral-wound membrane.

into the spacing material. The permeate stream flows toward the open edge at a 90° angle to the feed stream. The feed gas that does not permeate is collected as the residue stream. A large surface area per volume is obtained by placing a feed spacer on top of the leaf and rolling the membrane "sandwich" around the collection tube.

The fundamental model is based on the following assumptions [1]:

1. The feed stream contains a binary gas mixture.
2. Bulk flow and local permeation are described by a cross-flow pattern.
3. There is no pressure drop on the feed side.
4. The pressure drop on the permeate side is described by the Hagen–Poiseuille equation.
5. Membrane permeabilities are independent of pressure and concentration.
6. The porous supporting layer offers negligible resistance to gas flow.
7. There is no mixing in the porous support.
8. The permeate pressure varies only in the direction of permeate flow.

Several of these assumptions can be relaxed if necessary [6,9,16,17].

The fundamental model is comprised of three ordinary differential equations, two nonlinear algebraic equations, and one nonlinear integral equation. The differential equations describe the dependence of the dimensionless permeate pressure $\gamma(h)$, dimensionless permeate flow $\theta(h)$, and bulk permeate con-

centration $y(h)$ on the dimensionless leaf length variable h

$$\frac{d\gamma^2}{dh} = -C\theta \tag{1}$$

$$\frac{d\theta}{dh} = 1 - \frac{u_r}{u_f} \tag{2}$$

$$\frac{d(\theta y)}{dh} = x_f - x_r\frac{u_r}{u_f} \tag{3}$$

where u_f and $u_r(h)$ are the feed and residue flow rates per unit length, x_f and $x_r(h)$ are the feed and local residue concentrations, and:

$$C = \frac{2R_gT\mu LU_f}{g_cWtBP^2} \tag{4}$$

The differential equations are subject to mixed boundary conditions

$$\theta(0) = \theta(0)\,y(0) = 0 \tag{5}$$

$$\gamma(1) = \gamma_0 \tag{6}$$

where γ_0 is the ratio of the permeate and feed pressures at the permeate outlet.

The first nonlinear algebraic equation describes the relation between the local feed-side concentration $x(h,s)$ and the local permeate concentration on the membrane surface $y'(h,s)$

$$\frac{y'}{1-y'} = \frac{\alpha(x-\gamma y')}{1-x-\gamma(1-y')} \tag{7}$$

where α is the membrane selectivity and s is the dimensionless leaf width variable. The second algebraic equation describes the effect of the local permeate concentration on the feed-side flow rate per unit length $u(h,s)$

$$\frac{u}{u_f} = \left(\frac{y'}{y'_f}\right)^a\left(\frac{1-y'}{1-y'_f}\right)^b\left(\frac{\alpha-(\alpha-1)y'}{\alpha-(\alpha-1)y'_f}\right) \tag{8}$$

where $y'_f(h)$ is the local permeate concentration on the membrane surface at the feed inlet and:

$$a = \frac{\gamma(\alpha-1)+1}{(\alpha-1)(1-\gamma)}$$
$$b = \frac{\gamma(\alpha-1)-\alpha}{(\alpha-1)(1-\gamma)} \tag{9}$$

The nonlinear integral equation describes the relation between the dimensionless permeation factor

$$R = \frac{2WQ_2P}{du_f} = \frac{2WLQ_2P}{dU_f} \tag{10}$$

and the local permeate concentration:

$$R = \frac{1}{\alpha(1-\gamma)}\left\{\alpha-(\alpha-1)y'_f - \left[\alpha-(\alpha-1)y'_r\right]\frac{u_r}{u_f} - (\alpha-1)\int_{y'_f}^{y'_r}\left(\frac{u}{u_f}\right)_\gamma dy'\right\} \tag{11}$$

Note that the integration is performed at constant pressure.

For fixed operating pressures, the model can be solved if two flow rates and/or concentrations are specified. The standard case involves the calculation of the permeate flow rate and concentration for given feed conditions. The bulk residue flow rate and concentration then can be determined by material balances around the permeator. The fundamental model is difficult to solve as a result of the nonlinear differential-algebraic-integral equations and mixed boundary conditions. For the standard calculation problem, Pan [1] proposed an iterative solution technique based on the shooting method. However, this method is computationally expensive and therefore is not well suited for process design applications.

3. Approximate model

We propose an approximate modeling technique for spiral-wound gas permeators based on the fundamental model of Pan [1]. The key assumption is that the residue flow rate is constant in the direction of permeate flow, which implies that the permeate flow rate varies linearly along the direction of permeate flow. We show that this condition is satisfied approximately by the fundamental model under most operating conditions. The assumption is used to reduce the original boundary value problem to a small number of nonlinear algebraic equations that can be solved much more efficiently. In the Appendix, the

approximate modeling technique is compared to the one-point collocation method. Finally, a nonlinear programming method for estimating unknown parameters of the approximate model from experimental data is presented.

3.1. Model development

Fig. 2 shows predictions from the fundamental model for several feed concentrations and permeation factors. For each case, the dimensionless permeate flow rate θ and dimensionless residue flow rate u_r/u_f are plotted as a function of the dimensionless leaf length variable h. Note that u_r/u_f exhibits a very weak dependence on h, while θ essentially is a linear function of h. This trend is observed for a wide range of operating conditions. Motivated by this result, we assume that the residue flow rate u_r is

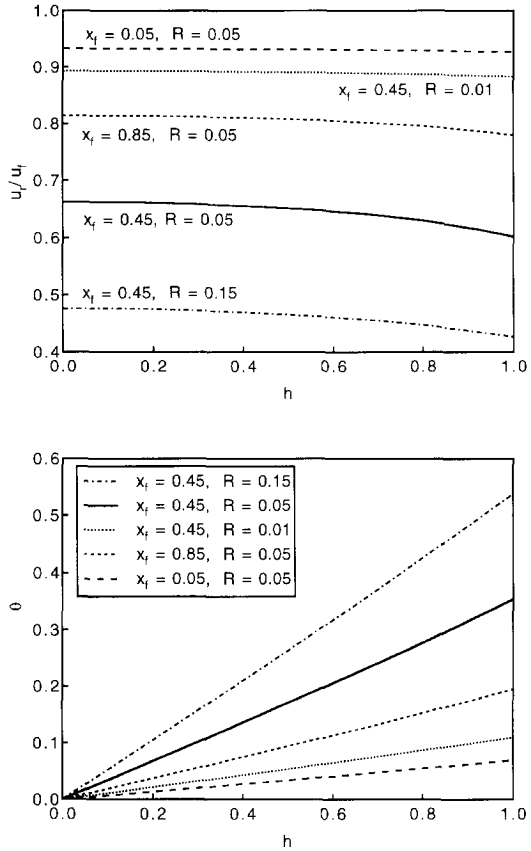

Fig. 2. Variations of the residue and permeate flow rates along the membrane length for the fundamental model.

independent of h. This assumption means that u_r does not vary along the direction of permeate flow, but it does not preclude u variations in the direction of feed flow (see Fig. 1). Under this condition, the differential Eq. (2) with boundary condition (5) is easily integrated:

$$\theta = \left(1 - \frac{u_r}{u_f}\right) h \tag{12}$$

Note that θ is a linear function of h, as expected. Substitution of (12) into (1) and integration with the boundary condition (6) yields:

$$\gamma^2 = \gamma_0^2 + \frac{1}{2} C \left(1 - \frac{u_r}{u_f}\right)(1 - h^2) \tag{13}$$

Note that we allow u_r to vary with h in the subsequent development. Thus, the assumption is invoked primarily to derive the approximate pressure distribution function (13).

The integral in (11) is evaluated as follows. We define the function in (8) as:

$$\phi(\gamma, y') \equiv \left(\frac{y'}{y'_f}\right)^a \left(\frac{1 - y'}{1 - y'_f}\right)^b \left(\frac{\alpha - (\alpha - 1) y'}{\alpha - (\alpha - 1) y'_f}\right) \tag{14}$$

It follows that:

$$\frac{u_r}{u_f} = \phi(\gamma, y'_r) \tag{15}$$

The integral is represented as

$$I(\gamma, y'_r) \equiv \int_{y'_f}^{y'_r} \left(\frac{u}{u_f}\right)_\gamma \mathrm{d}\, y' = \int_{y'_f}^{y'_r} \phi_\gamma(y') \mathrm{d}\, y' \tag{16}$$

where $\phi_\gamma(y')$ denotes that the integration is performed at constant pressure, and $\phi_\gamma(y'_f) = 1$. The integral is approximated using Gaussian quadrature [18]. The change of variable

$$\xi \equiv \frac{y' - y'_f}{y'_r - y'_f} \tag{17}$$

yields the expression

$$I(\gamma, y'_r) = (y'_r - y'_f) \int_0^1 \phi_\gamma(\xi) \mathrm{d}\, \xi \cong (y'_r - y'_f) \sum_{j=1}^{N} \phi_\gamma(y'_j) w_j \tag{18}$$

where N is the number of quadrature points, ξ_j and w_j are the quadrature points and weights, respectively, and $y'_j = y'_f + \xi_j(y'_r - y'_f)$. Thus, the integral Eq. (11) can be represented as:

$$R = \frac{1}{\alpha(1-\gamma)}\{\alpha - (\alpha-1)y'_f - [\alpha - (\alpha-1)y'_r]\phi(\gamma, y'_r) - (\alpha-1)I(\gamma, y'_r)\} \quad (19)$$

Simultaneous solution of (13), (15), (19), and (7) solved for y'_f with $x = x_f$ [1] at each quadrature point yields $\gamma(h_i)$, $u_r(h_i)/u_f$, $y'_r(h_i)$, and $y'_f(h_i)$. Here h_i represents the value of h at the ith quadrature point.

The nonlinear algebraic Eq. (7) can be rearranged as:

$$x_r = \frac{1 + \gamma(\alpha-1)(1-y'_r)}{y'_r + \alpha(1-y'_r)} y'_r \quad (20)$$

This allows the value of the residue concentration $x_r(h_i)$ at each quadrature point to be computed from $\gamma(h_i)$ and $y'_r(h_i)$. Material balances on a differential length of membrane yield,

$$u_f = u_r + v_a \quad (21)$$

$$u_f x_f = u_r x_r + v_a y'_a \quad (22)$$

where $v_a(h)$ and $y'_a(h)$ are the permeate flow rate per unit length and local permeate concentration, respectively, averaged over the entire width of the membrane. Therefore:

$$y'_a = \frac{x_f - x_r \frac{u_r}{u_f}}{1 - \frac{u_r}{u_f}} \quad (23)$$

The flow rate and concentration of the effluent permeate stream are calculated as follows. The flow rate is obtained from (2) using Gaussian quadrature

$$\theta_0 = 1 - \int_0^1 \frac{u_r}{u_f} dh \cong 1 - \sum_{i=1}^{M} \frac{u_r(h_i)}{u_f} w_i \quad (24)$$

where M is the number of quadrature points. By invoking the assumption that u_r is a "weak" function of h, it is easy to show that the permeate composition can be computed as:

$$y_0 = \int_0^1 y'_a dh \cong \sum_{i=1}^{M} y'_a(h_i) w_i \quad (25)$$

The flow rate η_0 and concentration x_0 of the effluent residue stream are determined from an overall material balance about the permeator:

$$\eta_0 = 1 - \theta_0 \quad (26)$$

$$x_0 = \frac{x_f - \theta_0 y_0}{1 - \theta_0} \quad (27)$$

The flow rates and concentrations of the effluent streams are easily calculated given the values $\gamma(h_i)$, $u_r(h_i)/u_f$, and $y'_r(h_i)$. Therefore, the original boundary value problem effectively is reduced to solution of the four nonlinear algebraic equations (7), (13), (15), and (19) at the quadrature points h_i. Solution complexity is not strongly affected by the number of quadrature points N used to approximate the integral in (18). By contrast, the four nonlinear algebraic equations must be solved simultaneously for each quadrature point used in the computation of the permeate flow rate and concentration. Our experience indicates that one quadrature point ($M = 1$) generally provides a satisfactory solution. In this case $h_1 = 0.5$ and $w_1 = 1$, and the quadrature formulas reduce to

$$\theta_0 = 1 - \frac{u_r(h_1)}{u_f} \quad (28)$$

$$y_0 = y'_a(h_1) = \frac{x_f - x_r(h_1)\frac{u_r(h_1)}{u_f}}{1 - \frac{u_r(h_1)}{u_f}} \quad (29)$$

where $u_r(h_1)$ and $x_r(h_1)$ are obtained by solving the four nonlinear algebraic equations at h_1.

It is interesting to note that the pressure distribution (13) has the following form in this case:

$$\gamma^2(h_1) = \gamma_0^2 + \frac{3}{8}C\left[1 - \frac{u_r(h_1)}{u_f}\right] \quad (30)$$

In the Appendix, we show that the approximate model with $M = 1$ is closely related to the model obtained when one-point collocation [18] is applied

to the fundamental model. The only difference is that the collocation method yields the following pressure distribution

$$\gamma^2(h_1) = \gamma_0^2 + \frac{1}{4}C\left[1 - \frac{u_r(h_1)}{u_f}\right] \tag{31}$$

where h_1 now is interpreted as the interior collocation point. The two relations are identical with the exception of the constant coefficient. While this appears to be a minor difference, the subsequent simulation results show that the proposed modeling technique can yield significant improvements in prediction accuracy.

3.2. Parameter estimation

A potential disadvantage of the proposed technique is that the approximate model contains all the parameters in the original fundamental model. In most applications, detailed characteristics of the permeator are not known at the preliminary design stage. Consequently, the approximate model may contain uncertain and/or unknown parameters. We present a nonlinear programming strategy [19–21] that provides a simple and efficient means of estimating unknown/uncertain model parameters from experimental data. The primary advantage of the proposed method is that nonlinear implicit equations can be handled. Although the estimation technique is presented for one-point quadrature, it is readily extended to the more general case.

The objective is to estimate model parameters associated with the internal characteristics of the permeator. We assume that the membrane selectivity α is known. Unknown parameters may include the membrane leaf length L, the leaf width W, the leaf thickness t, and the asymmetric membrane thickness d. Note that these four parameters appear in the approximate model only via the terms C (4) and R (10). However, these terms are not easily estimated since they also depend on the feed flow rate U_f and feed pressure P. This problem is handled by defining parameters that do not depend on the feed conditions:

$$C' \equiv \frac{P^2}{U_f}C \tag{32}$$

$$R' \equiv \frac{U_f}{P}R \tag{33}$$

Therefore, the problem is reduced to estimating the parameters C' and R'.

To facilitate parameter estimation, the model equations are formulated as follows. Eq. (28) is rearranged as:

$$\frac{u_r(h_1)}{u_f} = 1 - \theta_0 \equiv f_1(\theta_0) \tag{34}$$

Combining this result with (29), the residue concentration is expressed as:

$$x_r(h_1) = \frac{x_f - \theta_0 y_0}{1 - \theta_0} \equiv f_2(x_f, \theta_0, y_0) \tag{35}$$

The following relations are obtained from (7)

$$y_r'(h_1) = f_3[\gamma(h_1), x_r(h_1)] \tag{36}$$

$$y_f'(h_1) = f_3[\gamma(h_1), x_f] \tag{37}$$

where f_3 represents the function obtained when (7) is solved for y' [1]. The following result is obtained by combining (30) and (34):

$$\gamma^2(h_1) = \gamma_0^2 + \frac{3}{8}C\theta_0 \equiv f_4(\gamma_0, \theta_0, C) \tag{38}$$

Eq. (19) is represented as:

$$R = f_5[\gamma(h_1), y_f'(h_1), y_r'(h_1)] \tag{39}$$

The parameters C' and R' are estimated using a nonlinear programming approach. The measurement vector z and parameter vector ν are defined as:

$$z \equiv [x_f\ \gamma_0\ \theta_0\ y_0\ U_f\ P]^T \tag{40}$$

$$\nu \equiv [C'\ R']^T \tag{41}$$

Assume that N independent experiments are performed to generate the data set $\{z_1, z_2, \ldots, z_N\}$. Let $\hat{z}_i$ represent an estimate of the outcome of the ith experiment. The parameters are determined by solving the following minimization problem,

$$\min \Psi(\hat{z}_1, \ldots, \hat{z}_N, \nu) = \sum_{i=1}^{N} (\hat{z}_i - z_i)^T V_i^{-1} (\hat{z}_i - z_i) \tag{42}$$

subject to the constraints,

$$F(\hat{z}_i, \nu) = 0, \quad i = 1,2,\ldots,N \tag{43}$$

where V_i are covariance matrices, and F represents the vector function obtained from the scalar equa-

tions (34)–(39). In practice, the V_i are taken to be a constant, diagonal matrix with elements that reflect the relative accuracy of the measurements. It is important to note that reliable algorithms are available to solve the nonlinear optimization problem (42)–(43) [22,23]. A simpler estimation problem is obtained if the feed flow rate and pressure are held constant during the experiments. In this case, the parameters C and R can be estimated directly and the dimensionality of the problem is reduced:

$$z \equiv [x_f \; \gamma_0 \; \theta_0 \; y_0]^T \tag{44}$$

$$\nu \equiv [C \; R]^T \tag{45}$$

4. Results and discussion

We evaluate the approximate modeling technique via a case study of CO_2/CH_4 separations. The nominal model parameters and operating conditions for the spiral-wound permeator are shown in Table 1. These values do not correspond to any particular application, but the range of parameters considered cover a wide variety of CO_2/CH_4 separations. Note that a nominal value is not given for the feed pressure P because we work exclusively with the dimensionless model. The approximate modeling technique utilizes three quadrature points in the integral evaluation ($N = 3$) and one quadrature point in the computation of the effluent stream properties ($M = 1$). The resulting model is compared to the fundamental model and the model obtained using one-point collocation (see Appendix). The effectiveness of the parameter estimation strategy also is investigated.

Table 1
Nominal model parameters for case study

Parameter	Value	Variable	Value
x_f	0.45	θ_0	0.472
γ_0	0.05	y_0	0.844
α	30	η_0	0.528
C	0.1	x_0	0.099
R	0.1		

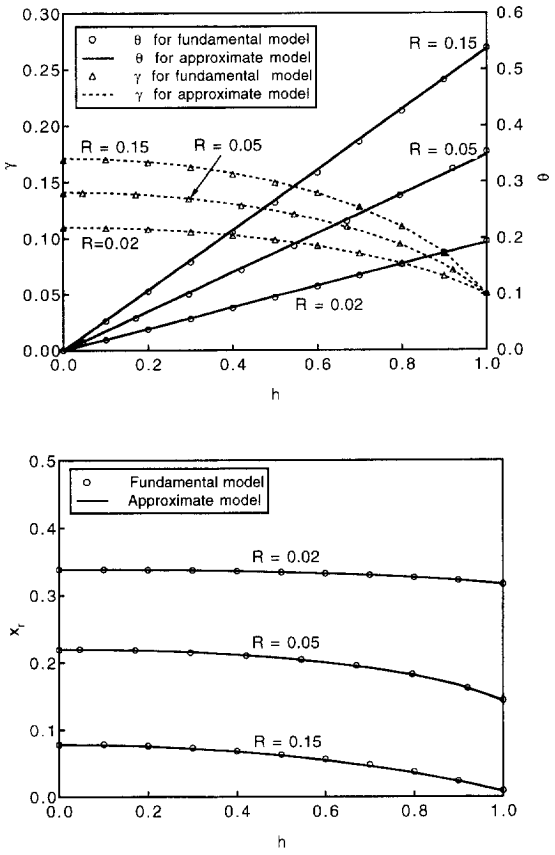

Fig. 3. Variations of the permeate pressure, permeate flow rate, and residue concentration along the membrane length.

4.1. Comparison to the fundamental model

The fundamental and approximate models are compared in Figs. 3–7. In each figure, parameters values that are not stated explicitly are given in Table 1. Fig. 3 shows the predicted permeate pressure γ, permeate flow rate θ, and residue concentration x_r as a function of the membrane length h for three value of the permeation factor R. The approximate model produces very accurate predictions of the spatial variations for each value of R. The effluent permeate flow rate θ_0 and effluent residue concentration x_0 for various combinations of R and the feed concentration x_f are shown in Fig. 4. The variable x_0 is shown rather that the effluent permeate concentration y_0 because the residue concentration exhibits larger variations and therefore is more

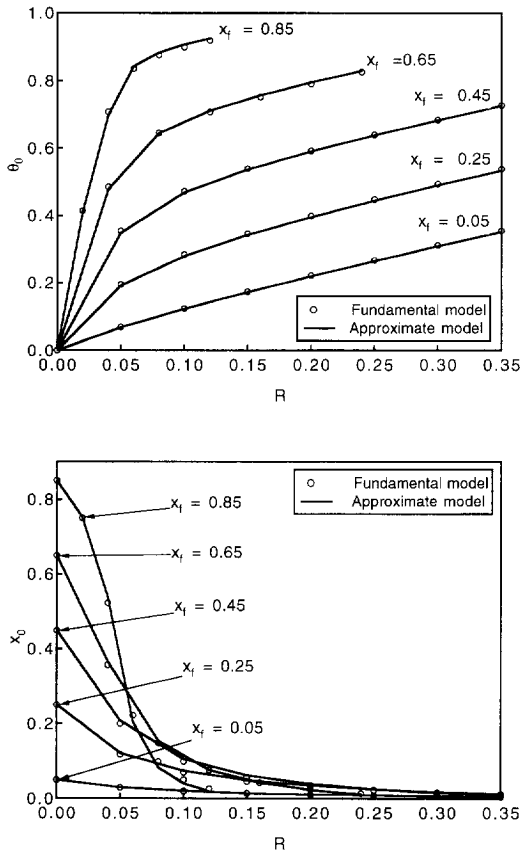

Fig. 4. Effect of the feed composition on the permeate flow rate and residue concentration.

illustrative. The approximate model yields accurate predictions of both variables for all operating conditions considered. It is interesting to note that higher feed compositions yield lower residue concentrations for large value of R. Consequently, results are not shown when both x_f and R assume large values because x_0 is close to zero under these conditions.

Fig. 5 shows the effluent permeate flow rate and residue concentration for several combinations of R and the permeate outlet pressure γ_0. The approximate model produces very accurate predictions for each case. The effect of R and the selectivity α on the effluent stream properties is shown in Fig. 6. The approximate model yields good predictions for all conditions considered, although small deviations between the two models are observed at intermediate values of α. Results are not shown for high values of α and R since x_0 is close to zero in this case.

Fig. 7 shows the effect of the parameters R and C on the effluent permeate flow rate and residue concentration. The approximate model produces good predictions for low values of C, but becomes slightly inaccurate as C increases. The result is expected because the approximation (13) is less valid when C assumes large values. Despite this discrepancy, the approximate model yields predictions that are sufficiently accurate for process design even for large values of C.

The results in Figs. 3–7 demonstrate that the approximate model provides accurate predictions over a wide range of operating conditions. The motivation for developing the approximate model is that the resulting nonlinear algebraic equations can be solved very efficiently. By contrast, the fundamental model consists of a set of nonlinear differential-algebraic-integral equations with mixed boundary condi-

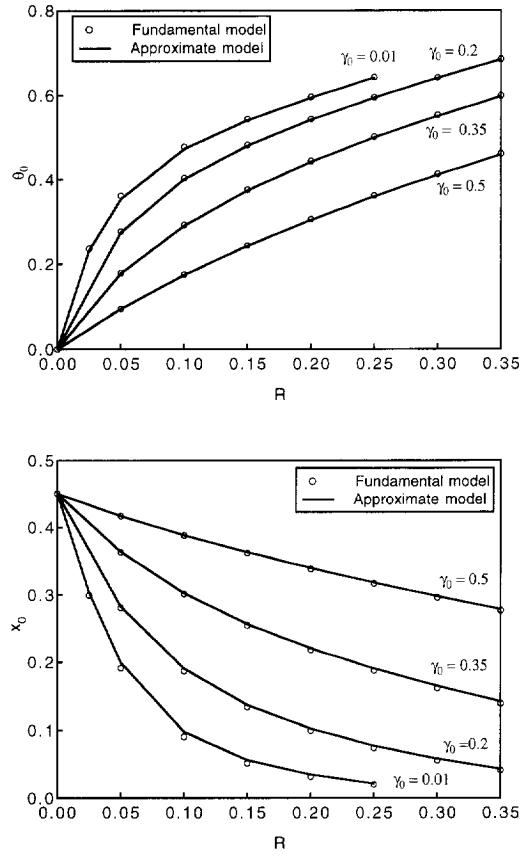

Fig. 5. Effect of the permeate pressure on the permeate flow rate and residue concentration.

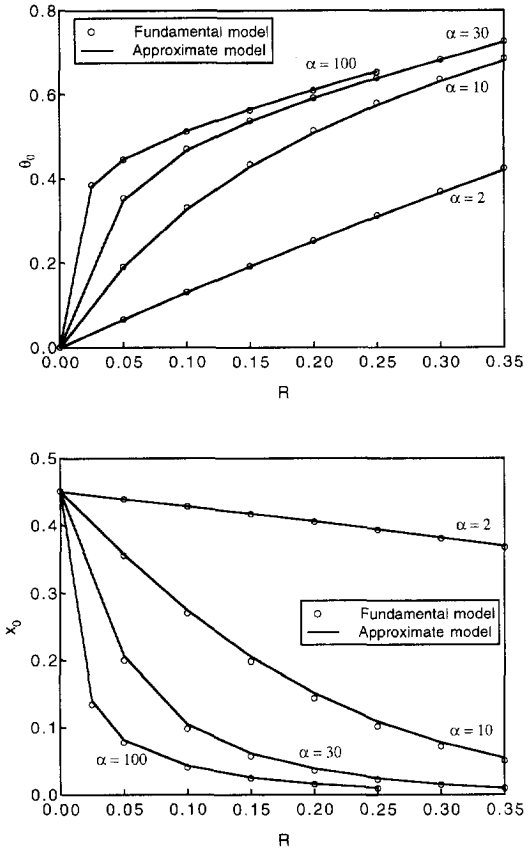

Fig. 6. Effect of the selectivity on the permeate flow rate and residue concentration.

tions. This model is solved using an iterative technique based on the shooting method [1]. Running MATLAB on an IBM RS-6000 workstation, we have found that the approximate model can be solved 200–400 times faster than the fundamental model. Consequently, the approximate model is well suited for process design studies.

4.2. Comparison to one-point collocation

Next we compare the proposed model to the approximate model obtained using one-point collocation (see Appendix). Results also are shown for the fundamental model to provide a basis for comparison. Fig. 8 shows the effluent permeate flow rate and residue concentration for several combinations of the feed concentration and permeation factor. Both approximate models yield good predictions, but the proposed model is slightly more accurate for some operating conditions. The effect of the parameters C and R on the effluent stream properties is shown in Fig. 9. While both models yield satisfactory results for small values of C, the proposed model is more accurate for large C values. In this case, more interior collocation points are required for an accurate solution. It is important to note that the accuracy of the proposed model also can be improved by increasing the number of quadrature points M. Consequently, the proposed method is preferred since both models require the same computing effort.

4.3. Parameter estimation

Finally, the effectiveness of the proposed parameter estimation strategy is investigated. As discussed previously, we assume that the membrane selectivity

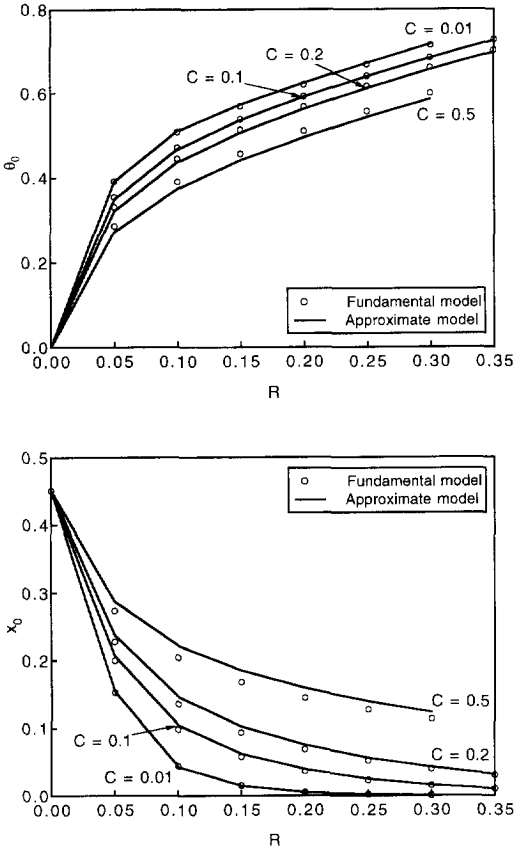

Fig. 7. Effect of the dimensionless constant C on the permeate flow rate and residue concentration.

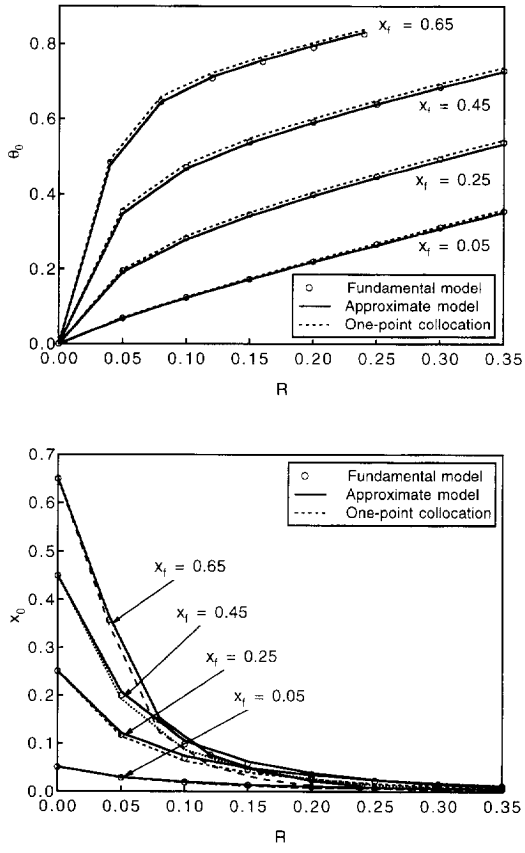

Fig. 8. Comparison of the approximate model and one-point collocation for different feed compositions.

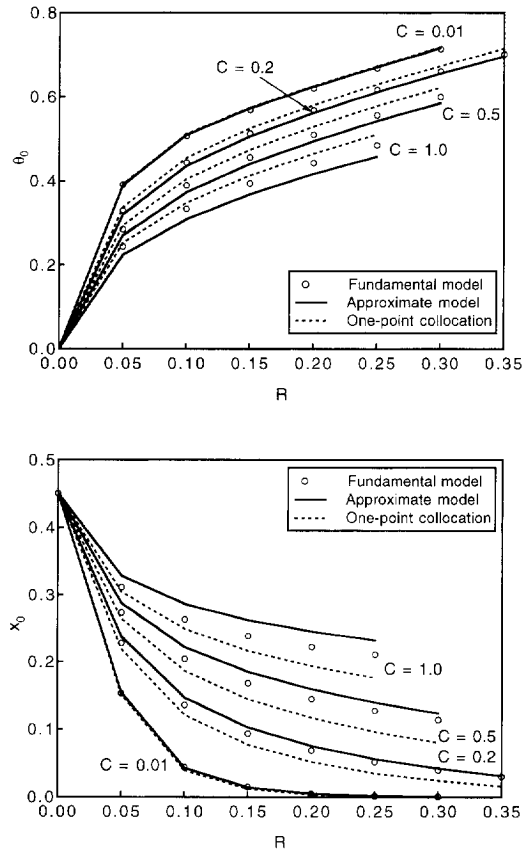

Fig. 9. Comparison of the approximate model and one-point collocation for different values of the dimensionless constant C.

α is known. Two data sets are collected by utilizing the fundamental model as the actual permeator. The feed concentration x_f and effluent permeate pressure γ_0 are varied systematically, while the feed flow rate U_f and feed pressure P are held constant. This allows the unknown model parameters ($C = 0.1$, $R = 0.1$) to be estimated directly. In the second data set, we add a randomly distributed signal with standard deviation $\sigma = 0.01$ to the measurements to simulate the effects of noise.

Table 2 shows the result of parameter estimation for nine independent sets of data without noise. The left-hand side of the table contains the measurements, while the right-hand side shows the estimated permeate stream properties obtained with the estimated parameters listed at the bottom of the table. The parameter R is identified almost perfectly, while $\hat{C}$ has an error of 10%. However, this discrepancy has very little effect on prediction accuracy. Parameter estimation for nine sets of data with noise is shown in Table 3, where the true values of the

Table 2
Parameter estimation using 9 data sets without noise

Data set	Measurements				Estimates	
	x_f	γ_0	θ_0	y_0	θ_0	y_0
1	0.2000	0.0500	0.2403	0.6470	0.2391	0.6457
2	0.2000	0.1000	0.2230	0.6313	0.2225	0.6305
3	0.2000	0.2000	0.1771	0.5755	0.1771	0.5751
4	0.4000	0.0500	0.4223	0.8201	0.4218	0.8191
5	0.4000	0.1000	0.4059	0.8182	0.4057	0.8174
6	0.4000	0.2000	0.3526	0.8076	0.3525	0.8073
7	0.6000	0.0500	0.6270	0.8939	0.6311	0.8909
8	0.6000	0.1000	0.6151	0.8952	0.6190	0.8926
9	0.6000	0.2000	0.5722	0.8974	0.5745	0.8962
			$\hat{C} = 0.0897$, $\hat{R} = 0.1001$			

Table 3
Parameter estimation using 9 data sets with noise

Data set	Measurements				Estimates	
	x_f	γ_0	θ_0	y_0	θ_0	y_0
1	0.2070	0.0556	0.2467	0.6474	0.2408	0.6666
2	0.1995	0.0987	0.2317	0.6065	0.2184	0.6414
3	0.2202	0.2055	0.1947	0.5871	0.1832	0.6153
4	0.4092	0.0390	0.4191	0.8099	0.4319	0.8314
5	0.3819	0.0927	0.4045	0.8297	0.3879	0.8154
6	0.4003	0.2140	0.3587	0.7998	0.3377	0.8118
7	0.5819	0.0438	0.6368	0.9003	0.6113	0.8911
8	0.6103	0.1024	0.6040	0.9034	0.6278	0.8999
9	0.6039	0.1841	0.5667	0.8957	0.5834	0.9015
	$\hat{C} = 0.0704$, $\hat{R} = 0.0948$					

measured variables are the same as in Table 2. The estimates $\hat{C}$ and $\hat{R}$ have errors of approximately 30% and 5%, respectively, and therefore the model predictions are slightly less accurate than in the noise-free case.

Table 4 shows the results of parameter estimation using ten experimental data sets from [24]. Binary CO_2/CH_4 data are generated from the original multicomponent data by considering the additional components (N_2 and hydrocarbons) as the slower permeating component (CH_4). Because the feed flow rate U_f and feed pressure P vary, it is necessary to estimate the parameters C' and R' rather than the dimensionless parameters. Note that the predictions are much less accurate than those obtained from the simulation data. This is expected since the experimental system has complications that are not present in simulation:

1. The separation is multicomponent.
2. There are differences in operating conditions that are not completely reflected in the experimental data sets (e.g. temperature variations).
3. The approximate model does not account for non-ideal effects such as concentration polarization, flow channelling, CO_2 plasticization, etc.

Nevertheless, predictions suitably accurate for preliminary process design are obtained by systematic estimation of the unknown model parameters.

5. Conclusions

An approximate modeling technique for spiral-wound permeators separating binary gas mixtures has been proposed and evaluated. The approach is based on the assumption that the residue flow rate is constant in the direction of permeate flow. The approximate model is derived by applying this assumption to an accepted fundamental model [1]. The original boundary value problem is reduced to a more tractable problem involving a small number of nonlinear algebraic equations. Additional justification for the modeling technique is obtained via comparison to one-point collocation. Because the approximate model may contain unknown/uncertain parameters, a nonlinear programming strategy for estimating parameters from experimental data has been

Table 4
Parameter estimation using experimental data from [24]

Data set	Measurements						Estimates	
	U_f (m^3/s)	P (MPa)	x_f	γ_0	θ_0	y_0	θ_0	y_0
1	0.0331	3.7557	0.0523	0.0272	0.3762	0.1318	0.3780	0.1338
2	0.0318	2.3767	0.0528	0.0429	0.2887	0.1564	0.2527	0.1726
3	0.0331	3.8247	0.1161	0.0267	0.4059	0.2676	0.4420	0.2570
4	0.0466	3.2041	0.1213	0.0318	0.3310	0.3345	0.2958	0.3550
5	0.0695	4.8589	0.1234	0.0210	0.3538	0.3319	0.3098	0.3609
6	0.0692	3.9626	0.1241	0.0258	0.2796	0.3732	0.2629	0.3930
7	0.0370	3.2386	0.1272	0.0315	0.3628	0.3212	0.3619	0.3266
8	0.0774	4.8589	0.1298	0.0210	0.3051	0.3766	0.2911	0.3927
9	0.0672	3.8936	0.1339	0.0262	0.2537	0.4081	0.2728	0.4114
10	0.0367	3.8936	0.2134	0.0262	0.5000	0.4115	0.5029	0.4164
	$\hat{C}' = 2.08 \times 10^{13}$ Pa^2 s/m^3, $\hat{R}' = 3.19 \times 10^{-9}$ m^3/Pa s							

proposed. A case study of CO_2/CH_4 separations has shown that the proposed model yields accurate predictions with considerably less computing time than the fundamental model. Future work will focus on the development of an approximate model for multicomponent separations and the use of the approximate models for membrane system design.

6. List of symbols

a	dimensionless constant defined by Eq. (9)
B	permeability of the spacing materials inside the spiral-wound leaf (m^2)
b	dimensionless constant defined by Eq. (9)
C	dimensionless constant defined by Eq. (4)
C'	constant defined by Eq. (32) (Pa^2 s/mol)
d	effective thickness of membrane (m)
g_c	Newton's law conversion factor
h	$= l/L$, dimensionless leaf length variable
h_i	quadrature points of h
l	membrane leaf length variable (m)
l_1, l_2	Lagrange interpolation polynomials
l'_1, l'_2	Lagrange interpolation polynomials
L	membrane leaf length (m)
M	number of quadrature points of θ_0 and y_0
N	number of quadrature points of the integral $I(\gamma, y'_r)$
	number of independent experiments in parameter estimation
P	feed-side pressure (Pa)
p	permeate-side pressure (Pa)
p_0	permeate outlet pressure (Pa)
Q_1	permeability of the more permeable component (mol/m s Pa)
Q_2	permeability of the less permeable component (mol/m s Pa)
R	dimensionless permeation factor defined by Eq. (10)
R'	constant defined by Eq. (33) (mol/Pa s)
R_g	ideal gas constant (m^3 Pa/kg mol K)
s	$= w/W$, dimensionless leaf width variable
t	membrane leaf thickness (m)
T	temperature (K)
U_f	feed gas flow rate per membrane leaf (mol/s)
U_0	residue gas flow rate per membrane leaf (mol/s)
u	feed-side gas flow rate per unit length of membrane leaf (mol/s m)
u_f	feed gas flow rate per unit length of membrane leaf (mol/s m)
u_r	residue gas flow rate per unit length of membrane leaf (mol/s m)
V	permeate flow rate (mol/s)
V_0	permeate flow rate at permeate outlet (mol/s)
V_i	covariance matrices in parameter estimation
v_a	permeate flow rate per unit length averaged over the width of the membrane (mol/s m)
W	membrane leaf width (m)
w	membrane leaf width variable (m)
w_i, w_j	quadrature weights
x	local feed-side concentration (mole fraction)
x_0	bulk residue stream concentration at outlet (mole fraction)
x_f	feed concentration (mol fraction)
x_r	local residue concentration along the outlet end of the membrane leaf (mole fraction)
y	permeate concentration in the bulk permeate stream (mole fraction)
y_0	permeate concentration in the bulk permeate stream at the permeate outlet (mole fraction)
y'	local permeate concentration on the membrane surface, (mole fraction)
y'_a	local permeate concentration averaged over the width of the membrane (mole fraction)
y'_f	local permeate concentration along the inlet end of the membrane leaf (mole fraction)
y'_j	local permeate concentrations at quadrature points (mole fraction)
y'_r	local permeate concentration along the outlet end of the membrane leaf (mole fraction)
z_i	experimental data sets expressed in Eq. (40)
$\hat{z}_i$	estimated data sets expressed in Eq. (40)
α	$= Q_1/Q_2$, membrane selectivity
γ	$= p/P$, ratio of permeate pressure to feed pressure
γ_0	$= p_0/P$, ratio of permeate pressure to feed pressure at the permeate outlet
μ	viscosity of gas mixture (Pa s)
θ	$= V/U_f$, ratio of permeate flow to feed flow
θ_0	$= V_0/U_f$, ratio of permeate flow to feed flow at permeate outlet

ξ_j standard quadrature points expressed in Eq. (17)
ϕ $= u/u_f$, function defined by Eq. (14)
η_0 $= U_0/U_f$, ratio of residue outlet stream flow to feed flow
ν estimated parameters expressed in Eq. (41)

Acknowledgements

Financial support from the Louisiana Quality Educational Support Fund (LEQSF(1993-96)-RD-B-03) is gratefully acknowledged.

Appendix A

We apply the one-point collocation method to the fundamental permeator model of Pan [1]. Only a brief presentation of the technique is provided here; detailed descriptions of the collocation method are available elsewhere [18,25]. The solution of the differential Eqs. (1)–(3) is approximated as

$$\gamma^2(h) \cong \gamma^2(h_1) l_1(h) + \gamma^2(h_2) l_2(h) \tag{46}$$

$$\theta(h) \cong \theta(h_1) l_1'(h) + \theta(h_2') l_2'(h) \tag{47}$$

$$\theta(h)\, y(h) \cong \theta(h_1)\, y(h_1) l_1'(h) + \theta(h_2')\, y(h_2') l_2'(h) \tag{48}$$

where the coefficients $\gamma(h_i)$, $\theta(h_i)$, and $y(h_i)$ are function values at the collocation point h_i, and $l_i(h)$ and $l_i'(h)$ are Lagrange interpolation polynomials. The first collocation point is $h_1 = 0.5$, and the second point is chosen according to the boundary condition as $h_2' = 0$ or $h_2 = 1$. The Lagrange polynomials are:

$$l_1(h) = \frac{h - h_2}{h_1 - h_2} = -2(h - 1) \tag{49}$$

$$l_2(h) = \frac{h - h_1}{h_2 - h_1} = 2(h - 0.5) \tag{50}$$

$$l_1'(h) = \frac{h - h_2'}{h_1 - h_2'} = 2h \tag{51}$$

$$l_2'(h) = \frac{h - h_1}{h_2' - h_1} = -2(h - 0.5) \tag{52}$$

The boundary conditions (5)–(6) are enforced as:

$$\gamma(h_2) = \gamma_0,\ \theta(h_2') = 0,\ \theta_2(h_2')\, y_2(h_2') = 0 \tag{53}$$

Therefore, the approximate solution is:

$$\gamma^2(h) \cong \gamma^2(h_1) l_1(h) + \gamma_0^2 l_2(h) \tag{54}$$

$$\theta(h) \cong \theta(h_1) l_1'(h) \tag{55}$$

$$\theta(h)\, y(h) \cong \theta(h_1)\, y(h_1) l_1'(h) \tag{56}$$

The derivatives of the Lagrange polynomials are:

$$\frac{\mathrm{d}l_1(h)}{\mathrm{d}h} = -2,\ \frac{\mathrm{d}l_2(h)}{\mathrm{d}h} = 2,\ \frac{\mathrm{d}l_1'(h)}{\mathrm{d}h} = 2 \tag{57}$$

By using the approximate solution to evaluate the derivatives, the differential Eqs. (1)–(3) are reduced to:

$$-2\gamma^2(h_1) + 2\gamma_0^2 = -C\theta(h_1) \tag{58}$$

$$2\theta(h_1) = 1 - \frac{u_r(h_1)}{u_f} \tag{59}$$

$$2\theta(h_1)\, y(h_1) = x_f - x_r(h_1)\frac{u_r(h_1)}{u_f} \tag{60}$$

These algebraic equations can be written as:

$$\gamma^2(h_1) = \gamma_0^2 + \frac{1}{4}C\left[1 - \frac{u_r(h_1)}{u_f}\right] \tag{61}$$

$$y(h_1) = \frac{x_f - x_r(h_1)\dfrac{u_r(h_1)}{u_f}}{1 - \dfrac{u_r(h_1)}{u_f}} \tag{62}$$

$$\theta(h_1) = \frac{1}{2}\left[1 - \frac{u_r(h_1)}{u_f}\right] \tag{63}$$

Similar to the proposed modeling technique, the values $y_f'(h_1)$, $\gamma(h_1)$, $u_r(h_1)/u_f$, and $y_r'(h_1)$ are determined via simultaneous solution of the nonlinear algebraic Eqs. (7), (61), (15), and (19). The effluent permeate flow rate is:

$$\theta_0 = \theta(h_1) l_1'(h_2) = 2\theta(h_1) = 1 - \frac{u_r(h_1)}{u_f} \tag{64}$$

The effluent permeate concentration is determined as:

$$y_0 = \frac{\theta(h_1)\, y(h_1)\, l_1'(h_2)}{\theta_0} = \frac{1}{2} y(h_1)\, l_1'(h_2) = y(h_1)$$

$$= \frac{x_f - x_r(h_1)\dfrac{u_r(h_1)}{u_f}}{1 - \dfrac{u_r(h_1)}{u_f}} \tag{65}$$

Note that the approximate models obtained with the proposed technique when $M = 1$ and one-point collocation are identical with the exception of the pressure distribution functions in (30) and (61).

References

[1] C.Y. Pan, Gas separation by permeators with high-flux asymmetric membranes, AIChE J., 29 (1983) 545–552.

[2] R.W. Spillman, Economics of gas separation membranes, Chem. Eng. Prog., January (1989) 41–62.

[3] W.J. Koros and G.K. Fleming, Membrane-based gas separation, J. Membrane Sci., 83 (1983) 1–80.

[4] R.R. Zolandz and G.K. Fleming, Gas permeation, in W.H. Ho and K.K. Sirkar (Eds.), Membrane Handbook, Van Nostrand and Reinhold, NY, 1989, Chap. II.

[5] W.J. Koros and R.T. Chern, Separation of gaseous mixtures with polymer membranes, in R.W. Rousseau (Ed.), Handbook of Separation Process Technology, Wiley-Interscience, New York, 1987, Chap. 20.

[6] A.S. Kovvali, S. Vemury, K.R. Krovvidi and A.A. Khan, Models and analyses of membrane gas permeators, J. Membrane Sci., 73 (1992) 1–23.

[7] S. Weller and W.A. Steiner, Engineering aspects of separation of gases, Chem. Eng. Prog., 46 (1950) 585.

[8] D.W. Brubaker and K. Kammermeyer, Separation of gases by plastic membranes: Permeation rates and extent of separation, Ind. Eng. Chem., 46 (1954) 733.

[9] R.T. Chern, W.J. Koros and P.S. Fedkiw, Simulation of a hollow-fiber separation: The effects of process and design variables, Ind. Eng. Chem. Des. Dev., 24 (1985) 1015–1022.

[10] C.Y. Pan, Gas separation by high-flux, asymmetric hollow-fiber membrane, AIChE J., 32 (1986) 2020–2027.

[11] K. Li, D.R. Acharya and R. Hughes, Mathematical modelling of multicomponent membrane permeators, J. Membrane Sci., 52 (1990) 205–219.

[12] K.R. Krovvidi, A.S. Kovvali, S. Vemury and A.A. Khan, Approximate solutions for gas permeators separating binary mixtures, J. Membrane Sci., 66 (1992) 103–118.

[13] T. Pettersen and K.M. Lien, A new robust design model for gas separating membrane modules based on analogy with counter-current heat exchangers, Computers Chem. Eng., 18 (1994) 427–439.

[14] A.S. Kovvali, S. Vemury and W. Admassu, Modeling of multicomponent countercurrent gas permeators, Ind. Eng. Chem. Res., 33 (1994) 896–903.

[15] H. Chen, G. Jiang and R. Xu, An approximate solution for countercurrent gas permeation separating multicomponent mixtures, J. Membrane Sci., 95 (1994) 11–19.

[16] Y. Shindo, T. Hakuta, H. Yoshitome and H. Inoue, Calculation methods for multicomponent gas separation by permeation, Sep. Sci. Technol., 20 (1985) 445–459.

[17] A.G. Narinsky, Applicability conditions of idealized flow models for gas separation by asymmetric membrane, J. Membrane Sci., 55 (1991) 333–347.

[18] R.G. Rice and D.D. Do, Applied Mathematics and Modeling for Chemical Engineers, Wiley, New York, NY, 1995.

[19] H.I. Britt and R.H. Luecke, The estimation of parameters in nonlinear, implicit models, Technometrics, 15 (1973) 233–247.

[20] I.-W. Kim, M.J. Liebman and T.F. Edgar, Robust error-in-variables estimation using nonlinear programming techniques, AIChE J., 36 (1990) 985–993.

[21] V.G. Dovi, A.P. Reverberi and L. Maga, Optimal design of sequential experiments for error-in-variables models, Comput. Chem. Eng., 17 (1993) 111–115.

[22] A. Brooke, D. Kendrick and A. Meeraus, GAMS: A User's Guide, Scientific Press, Palo Alto, CA, 1992.

[23] C.A. Floudas, Nonlinear and Mixed-Integer Optimization, Scientific Press, Oxford, 1995.

[24] A.L. Lee and H.L. Feldkirchner, Development of a Database for Advanced Processes to Remove Carbon Dioxide From Subquality Natural Gas, Topical Report GRI-93/0247, Gas Research Institute, 1993.

[25] B.A. Finlayson, Nonlinear Analysis in Chemical Engineering, McGraw-Hill, New York, 1980.